Automotive Experiences
Vol. 8 No. 1 (2025) pp. 32-45
p-ISSN: 2615-6202 e-ISSN: 2615-6636

Research Paper

Modeling the Dynamics of a Passenger Car Using Experimental Data on Nonlinear Passive Shock Absorbers

Avicenna An-Nizhami, Yusuf Dewantoro Herlambang, Nanang Apriandi, Bono, Friska Ayu Fitrianti Sugiono, Ali Sai'in, Ignatius Gunawan Widodo, Padang Yanuar

Department of Mechanical Engineering, Politeknik Negeri Semarang, Semarang 50275, Indonesia

masyusufdh@polines.ac.id

https://doi.org/10.31603/ae.12792

Published by Automotive Laboratory of Universitas Muhammadiyah Magelang

Article Info
Submitted:
09/12/2024
Revised:
21/01/2025
Accepted:
08/03/2025
Online first:
09/03/2025

Abstract

This study explores the dynamic response of passenger cars equipped with nonlinear passive shock absorbers, emphasizing the nonlinear damping characteristics over traditional linear models in simulating real-world driving conditions. To capture the nonlinear damping behavior, experimental data from a shock absorber testing apparatus was utilized to derive an empirical formula. The damping force was modeled using a seventh-order polynomial equation, accurately representing the force-velocity relationship. This nonlinear damping model was integrated into a half-car suspension model, which was subjected to simulations involving two road profiles: a bump and an irregular sinusoidal road profile. Simulations demonstrated that the nonlinear model outperformed its linear counterpart, particularly in vibration control. It achieved significant reductions in body displacement, body acceleration, and suspension deflection, with notable improvements at resonance speeds. Root Mean Square (RMS) analysis further corroborated the nonlinear model's superior damping performance, showing lower displacement and acceleration values compared to the linear model. The findings indicate the effectiveness of nonlinear damping models in enhancing ride comfort and vehicle stability, providing a more realistic and effective framework for vehicle dynamic analysis compared to conventional linear approaches.

Keywords: Nonlinear damping; Shock absorber; Dynamic response; Vibration control; Suspension system; Empirical formula

1. Introduction

The dynamic response of a vehicle, particularly when subjected to external excitations from specific road conditions, is critical to assuring ride comfort, vehicle stability, and overall road safety. The suspension system is a critical component in meeting these requirements. The shock absorber is a critical component of the suspension system that provides damping forces to reduce undesirable vibrations induced by road disturbances. The investigation of the dynamic response of cars subjected to this disturbance can lead to better suspension design, which improves ride comfort and handling performance. Comfort and road handling performance are usually determined by the characteristics of the shock absorber. Shock absorbers are often characterised by a damping force-velocity diagram. In the case of a linear model of a shock absorber, the force exerted by the shock absorber is proportional to its velocity relative motion. This implies a straightforward relation between force and velocity, which is easier to model. Real-world suspension systems, on the other hand, frequently exhibit nonlinear damping behaviour, with a more complicated force-velocity relationship. Non-linear models are better at capturing a vehicle's true behaviour under operating settings when linear models fail to predict the response appropriately. Thus, the analysis of the nonlinear behaviour of shock absorbers and its impact on vehicle dynamics is critical to advance the design and development of next-generation suspension.

Nomenclature		
M	Sprung mass of the vehicle	kg
M_w	Unsprung mass of the vehicle	kg
k	Suspension spring stiffness	N/m
c	Shock absorber damping coefficient	N·s/m
k_t	Tire stiffness	N/m
l_1	Distance from the center of gravity to the front suspension	m
l_2	Distance from the center of gravity to the rear suspension	m
y	Vertical displacement of the vehicle body	m
$\ddot{y}$	Vertical acceleration of the vehicle body	m/s²
$\dot{y}$	Vertical velocity of the vehicle body	m/s
F_D	Damping force of the shock absorber	N
v_1, v_2	Suspension deflection velocities for front and rear, respectively	m/s
$a_1, a_2, \ldots, a_8$	Coefficients in the seventh-order polynomial describing nonlinear damping force	Dimensionless
$w(x)$	Road height as a function of distance	m
bh	Bump height of the road profile	m
bp	Bump position of the road profile	m
bw	Bump width of the road profile	m
A_i	Amplitude of irregular sinusoidal road profile	m
f_i	Frequency of irregular sinusoidal road profile	Hz
ϕ_i	Phase angle of sinusoidal components	rad
RMS	Root Mean Square value	Dependent on context

Extensive studies have been conducted to predict the dynamic response of the vehicle and the optimization of ride comfort. Studies on the dynamic response of the vehicle have been conducted with various models such as the quarter-car model [1], [2], [3], [4], [5], half-car model [6], [7] and full car model [8], [9]. Several types of research to improve vehicle dynamic response have been studied. One way to improve the dynamic response on passive suspension was implementing a modified twin-tube shock absorber [10] or using a secondary suspension system as cabin suspension [11]. The other way is to use semi-active suspension where one of the suspension components adapts depending on the road condition. Various control strategies have been implemented for semi-active suspension. Skyhook, ground hook, and hybrid control have been implemented on the semi-active suspension and improved further by using modified sky hook control by Koulocheris et al. [12]. In order to further obtain a more desirable dynamic response, an active suspension system was implemented on a vehicle. An active suspension system works by actively controlling the movement of the wheel and cassis in real-time using a hydraulic or pneumatic actuator. The major drawback of the active suspension system is the amount of power source required to operate. Various controller strategies have been intensively studied to improve dynamic response or increase efficiency. A control strategy namely adaptive event-triggered dynamic output feedback control has been implemented on the active suspension system by Wong et al. [13] to enhance performance and efficiency. Pedro et al. [14] proposed a Model Predictive Controller (MPC) for a half-car active suspension system, the dynamics results show that the proposed model outperforms passive suspension. Elwahab et al. [15] presented an approach to the performance of an active suspension system using Linear Quadratic Regulator (LQR), PID, and H-infinity control strategies for passenger vehicles. Khan et al. [16] proposed a half-car model incorporating Feedback Linearization and an LQR Controller design for an active suspension system. Unguritu et al. [17] developed a control strategy, namely Adaptive Harmonic Control (AHC), for an active suspension system on a half-car model. Armansyah [18] introduced an RMS-based optimization methodology to refine air suspension systems for enhanced ride comfort and handling in road vehicles. The proposed model reveals significant reductions in sprung mass acceleration and improved handling stability.

Several studies have been conducted on the nonlinear characteristics of shock absorbers. Hryciów [19] conducted a study that exhibits the

strong nonlinear characteristic of shock absorbers concerning temperature, the results show that the relationship between temperature and damping characteristics is nonlinear, especially at extreme temperatures. Barethiye et al. [20] focus on capturing the complex nonlinear and hysteresis behaviors of shock absorbers used in vehicle suspension systems. Chen et al. [21] introduced a systematic modeling methodology grounded in the coupled nonlinear dynamics of suspension systems addressing passenger comfort. Ke et al. [22] introduced a design methodology for nonlinear stiffness composite helical springs. Finite element models were developed and analyzed using ABAQUS software. Silveira et al. [23] investigated the dynamic characteristics of vehicle suspension systems incorporating asymmetrical viscous damping. Prior research highlights the benefits of asymmetrical dampers in improving ride quality. Mohanty et al. [24] presented an analysis of a single-degree-of-freedom spring-mass-damper primary system. The Method of Multiple Scales (MMS) is employed to derive the system response in the nonlinear case and compare it with the linear analysis. Ning Zhang et al. [25] examined the dynamic stability of car-trailer combinations incorporating nonlinear damper properties. A significant limitation of these studies lies in their reliance on numerically derived nonlinear models for shock absorber damping and spring stiffness, based solely on design specifications. However, the mathematical representation of damping force nonlinearity, based on experimental data from actual shock absorbers, has been largely overlooked. Consequently, the investigation of vehicle dynamics incorporating experimentally derived nonlinear shock absorber characteristics remains an underexplored area, despite the distinct divergence from the predictions of conventional linear models. Therefore, this study aims to investigate the nonlinear characteristics of shock absorbers and their implications on the dynamic response of a vehicle. The nonlinear properties of shock absorbers are examined through experimental methods, and the experimental data is then captured and processed to derive an empirical equation. The damping force empirical equation was then used as a nonlinear model of the shock absorber. The impact of the nonlinear damping force on the vehicle's dynamic response is analyzed under two distinct road profile inputs.

2. Method

2.1. Experimental Setup for Car Shock Absorber

In order to obtain the relationship data between damping force and velocity of car shock absorber, an experiment was carried out on our shock absorber testing apparatus. The shock absorber being tested was used in the Karimun car from the Suzuki factory in Indonesia. The experimental setup is shown in **Figure 1**. The testing apparatus shown includes a shock absorber specimen also force and frequency sensors to measure the damping force under various velocity conditions. The shock absorber is subjected to a sinusoidal motion in various frequencies to cover a range of velocities. The experiments begin with the shock absorber mounted between the dynamic actuator and a fixture and then subjected to an incremental increase in velocity generated by the actuator. In order to ensure reliability, the experiment was conducted multiple times under identical conditions and the results were averaged.

The damping force data was plotted against velocity data to visualize the relationship between the two variables. The shape of the graph indicates

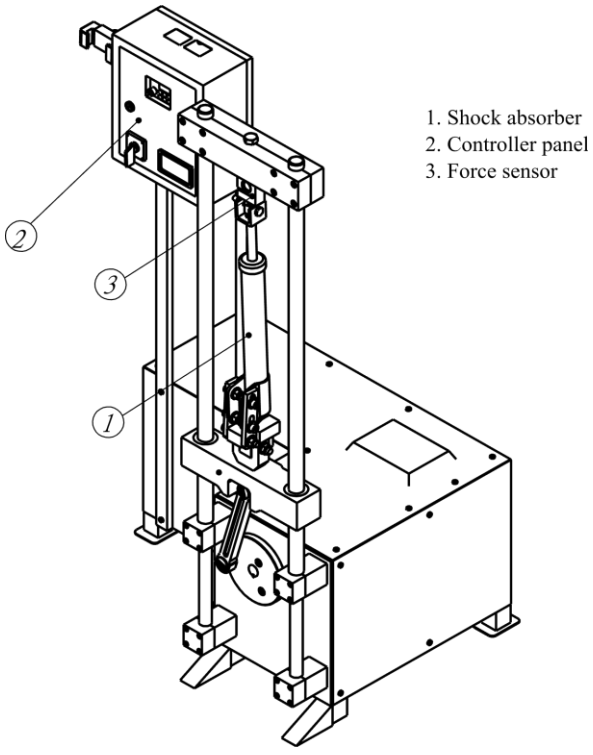

Figure 1. Experimental set-up on car shock absorber

whether the relationship is linear or nonlinear. A curve-fitting algorithm was implemented to obtain the best-fit equation to describe the relationship between damping force and velocity. The accuracy of the empirical equation was validated using the experiment data.

2.2. *Half-car Model*

A half-vehicle suspension system model was developed (see **Figure 2**), including five degrees of freedom (5 DoF). The model is described as a set of ordinary differential equations (ODE) shown in Eq. (1)-(4) based on the formulation by Jonjo et al. [3], the dot notation indicates the derivative taken with respect to time. The vehicle dynamics equation left-hand side (LHS) is the sum of vertical force exerted on the mass, while the right-hand side (RHS) is the dynamic motion or the inertial force of the mass. The simulation parameters, including vehicle mass, spring constants, and initial conditions, were defined based on typical values for a standard passenger car described in **Table 1**.

In this context (Eq. (1)-(4)), M represents the sprung mass, M_w represents the unsprung mass. While $\ddot{y}$, $\dot{y}$, and y refers to the vertical acceleration, velocity, and displacement of the vehicle body, respectively, F_D represents the damping force of the shock absorber, and k and c correspond to the suspension spring stiffness and the shock absorber damping coefficient, respectively. To solve the dynamic equations, we employed the Dormand-Prince time integration method, which was previously validated in an earlier study [26].

The block diagram shown in **Figure 3** describe the dynamics of a vehicle suspension system responding to road disturbances. Road irregularities act as inputs, affecting the front and rear unsprung masses (wheels and associated components). These forces are transmitted to the front and rear suspension systems, which consist of springs and dampers designed to absorb and reduce vibrations. The suspension systems then interact with the sprung mass (the vehicle body), influencing its vertical acceleration, displacement, and suspension deflection.

The nonlinear model of the shock absorber damping force formula is different from the linear model, the nonlinear and linear model formulations are described in Eq. (5) for the linear model and Eq. (6) and (7) for the nonlinear model. The nonlinear model is described as a seventh-order polynomial equation.

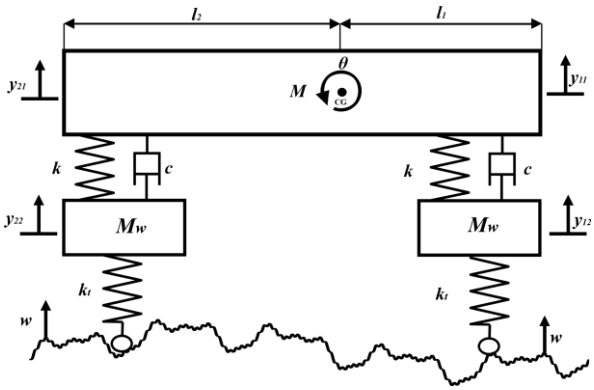

Figure 2. Half-vehicle suspension system

Table 1. Parameters used in the half-car model

Symbol	Value
M	835 [kg]
M_w	50 [kg]
k	52,250 [N/m]
c	2417.42 [N.s/m]
k_t	120,000 [N/m]
l_1	1.1 [m]
l_2	1.2 [m]

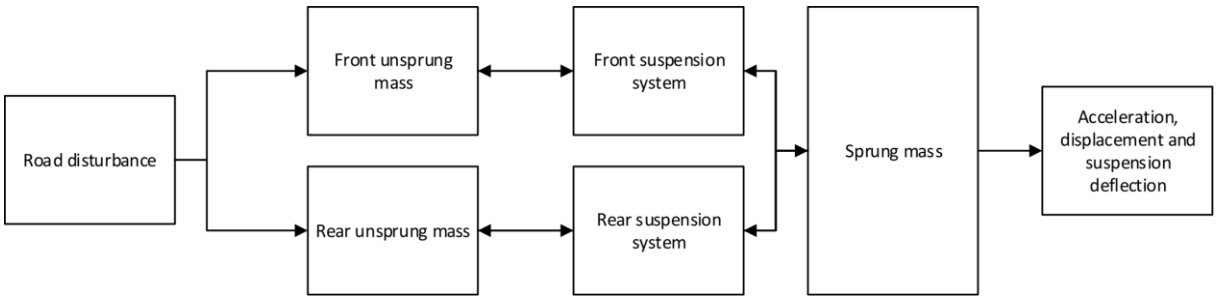

Figure 3. Block diagram of the equation flow

$$k(y_{12} - y_{11} - \theta l_1)l_1 + F_{D_{11}} l_1 - k(y_{22} - y_{21} - \theta l_2)l_2 - F_{D_{21}} l_2 = I\ddot{\theta} \quad (1)$$

$$k(y_{12} - y_{11} - \theta l_1) + F_{D_{11}} + k(y_{22} - y_{21} - \theta l_2) + F_{D_{21}} = M\ddot{y}_c \quad (2)$$

$$k_t(w_f - y_{12}) - k(y_{12} - y_{11} - \theta l_1) - F_{D_{11}} = M_w\ddot{y}_{12} \quad (3)$$

$$k_t(w_r - z_{22}) - k(y_{22} - y_{21} - \theta l_2) - F_{D_{11}} = M_w\ddot{y}_{22} \quad (4)$$

$$F_{D_{11}} = cv_1 \text{ and } F_{D_{21}} = cv_2 \quad (5)$$

$$F_{D_{11}} = a_1v_1^7 + a_2v_1^6 + a_3v_1^5 + a_4v_1^4 + a_5v_1^3 + a_6v_1^2 + a_7v_1 + a_8 \quad (6)$$

$$F_{D_{21}} = a_1v_2^7 + a_2v_2^6 + a_3v_2^5 + a_4v_2^4 + a_5v_2^3 + a_6v_2^2 + a_7v_2 + a_8 \quad (7)$$

In this context v_1 and v_2 are suspension deflection velocity, where $v_1 = \dot{y}_{12} - \dot{y}_{11} - \dot{\theta}l_1$ and $v_2 = \dot{y}_{22} - \dot{y}_{21} - \dot{\theta}l_2$. The empirically derived formula for the damping force was integrated into the suspension model, replacing the standard linear damping model typically used in vehicle dynamic simulations. The value of a_{1-8} are shown in **Table 2**.

2.3. Road Profile

A road profile can be described as the fluctuating elevation or displacement of the road's surface, which shifts based on the distance a vehicle covers. In this context, two distinct road profiles are created: one is a singular bump, while the other is an irregular sinusoidal wave. These road profiles were modeled to simulate several road conditions. The bump captured a sudden rise in the elevation, simulating real-life road profiles such as speed bumps or potholes. The irregular sinusoidal profile represents rough surfaces, offering a realistic representation of rugged or bumpy terrain. The road profiles are described in equations denoted in Eq. (8) for bump road profile and Eq. (9) for irregular sinusoidal road profile. The graphical representation of the road profiles is depicted in **Figure 4a** for the bump road profile and **Figure 4b** for the irregular sinusoidal road profile.

Table 2. The value of a_{1-8} for the nonlinear model of the shock absorber

Symbol	Value
a_1	-3.032×10^4
a_2	3.373
a_3	3.154×10^4
a_4	-2.175×10^{-11}
a_5	-1.14×10^4
a_6	3.685×10^{-12}
a_7	3135
a_8	-1.039×10^{-13}

$$w(x) = bh \times \exp\left(-\frac{(x - bp)^2}{2 \times (bw/2)^2}\right) \quad (8)$$

$$w(x) = \sum_{i=1}^{N} A_i \sin(2\pi f_i x + \phi_i) \quad (9)$$

In this context, $w(x)$ represents the road height as a function of the road distance x. For bump road profile, bh represents bump height, bp represents bump position, and bw represents bump width. While for irregular sinusoidal road profile, A_i denotes the amplitude of road height with multiple values of [0.005, 0.003, 0.002, 0.001, 0.0005] meters. Similarly, f_i refers to the frequency with corresponding values of [0.1, 0.5, 1, 2, 10] Hz.

3. Result and Discussion

This section presents the findings of the study, organized into three subsections. The first subsection provides an examination of the experimental results and their comparison with the mathematical model of the shock absorber. The second subsection explores the vehicle's dynamic response to a bump road profile, while the final subsection analyzes the vehicle's response to an irregular sinusoidal road profile. The results are presented in both the time domain and the frequency domain (for the irregular sinusoidal road profile) to offer comprehensive insights.

3.1. Comparing Experimental Data to Linear and Nonlinear Models

Figure 5 shows the comparison of the experimental damping force data and the mathematical model of linear and nonlinear approaches for the same shock absorber. The linear model was derived from the average damp-

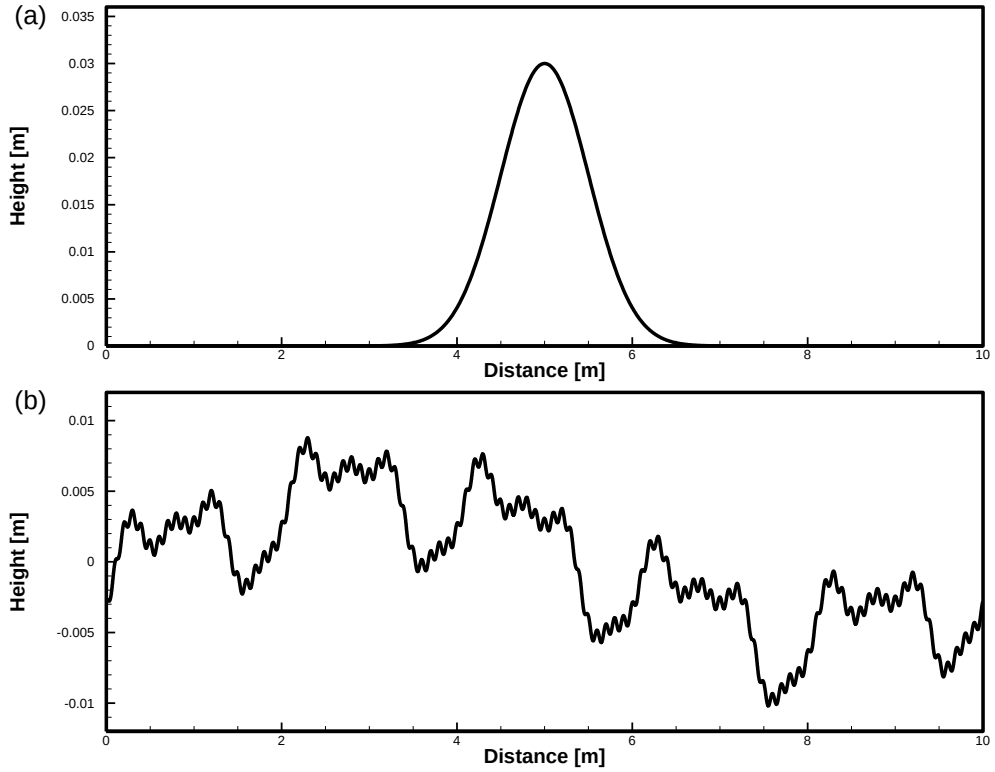

Figure 4. Road profiles: (a) Bump road profile; (b) Irregular road profile

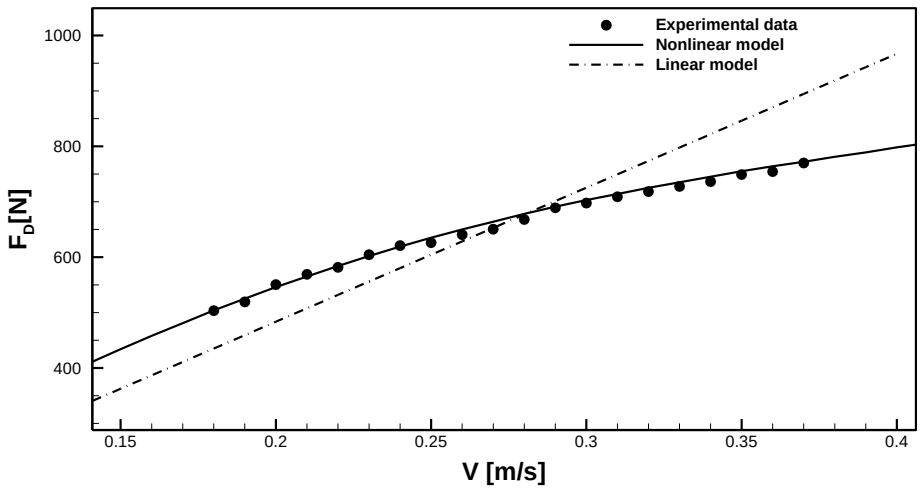

Figure 5. Comparison of the damping force to the velocity of the shock absorber

-ing coefficient of the experimental data. The nonlinear model was derived from data fitting using the sum of least square method to obtain the seventh-order polynomial equation. The horizontal axis represents velocity, V, while the vertical axis represents the damping force, F_D. The solid black line represents the nonlinear model, the dashed line shows the linear model, and the dot symbols correspond to the experimental data.

The comparison indicates that the nonlinear damping model is a more accurate representation of the damping force experienced in the experimental setup. These results highlight the limitations of linear models in capturing the complex, force-velocity characteristic of passive shock absorbers, suggesting the need for nonlinear formulations in vehicle dynamics modeling to improve accuracy in predicting vehicle dynamics motion.

3.2. Vehicle Dynamics Response with Bump Road Profile

When analyzing the dynamic response of a vehicle body to a bump road profile at different

vehicle velocities, time-domain graphs of acceleration, displacement, and damping force are required to comprehensively analyze how the vehicle interacts with the road and how the suspension system responds to different speeds. Each graph will have four curves, corresponding to different velocities (2.5 m/s, 5 m/s, 7.5 m/s, and 10 m/s), for a representation of how speed influences the vehicle's dynamic behavior.

The time history of acceleration is depicted in **Figure 6**. The graph captures the vertical acceleration of the vehicle body as it passes the bump. The acceleration for linear and nonlinear models is depicted in different types of lines, the solid black line shows a nonlinear model while the red dashed line shows a linear model. The acceleration graphs indicate that the maximum peak increases as the vehicle velocity increases. The maximum peak for all vehicle velocities is delayed where it occurs with a negative value at the second peak for both models, indicating the peak occurs after the vehicle passes the bump. At 2.5 m/s and 5 m/s, the linear model shows a higher acceleration peak and takes longer for the oscillation to decay, indicating efficient damping for the nonlinear model. Conversely, at 7.5 m/s and 10 m/s, the maximum acceleration of the linear model closely follows the nonlinear model with a slightly lower peak. However, for all velocities, the acceleration for the nonlinear model takes a shorter time to decay. This suggests that the nonlinear suspension system becomes increasingly important in dissipating energy as the vehicle encounters the bump.

Figure 7 shows the time history of vehicle body displacement of both models, linear (dashed red line) and nonlinear (solid black line) models of the shock absorber. Opposing the body acceleration, the maximum displacement decreases as the velocity increases. At a lower speed of 2.5 m/s, the linear model shows higher initial body displacement and more pronounced oscillation compared to the nonlinear model. The nonlinear model at all velocities has a faster rate of reaching stability compared to the linear model. This indicates that the linear damper does not dissipate energy as efficiently in this case, allowing the vehicle body to oscillate more freely. In contrast, the nonlinear damper exerts greater resistance, limiting the motion and damping the oscillations

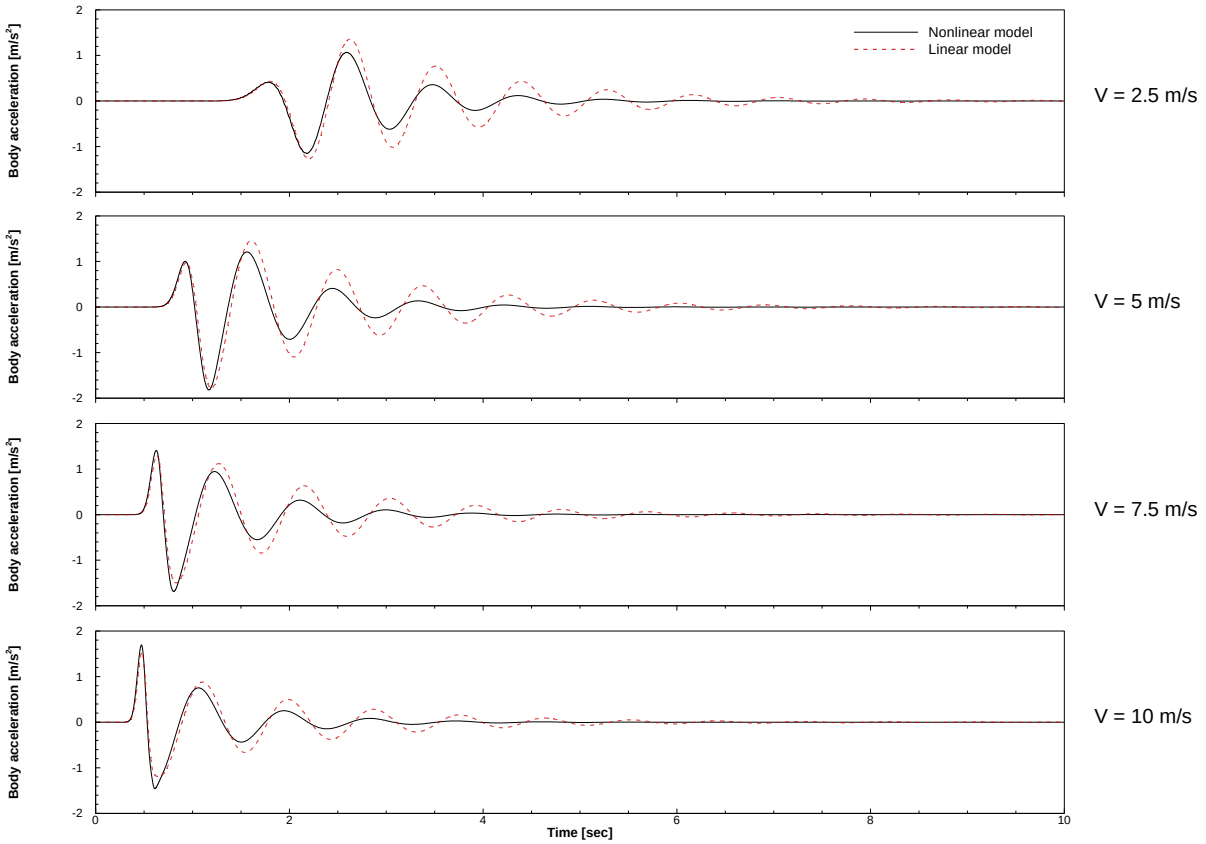

Figure 6. Vehicle body acceleration ($\ddot{y}$) for bump roads

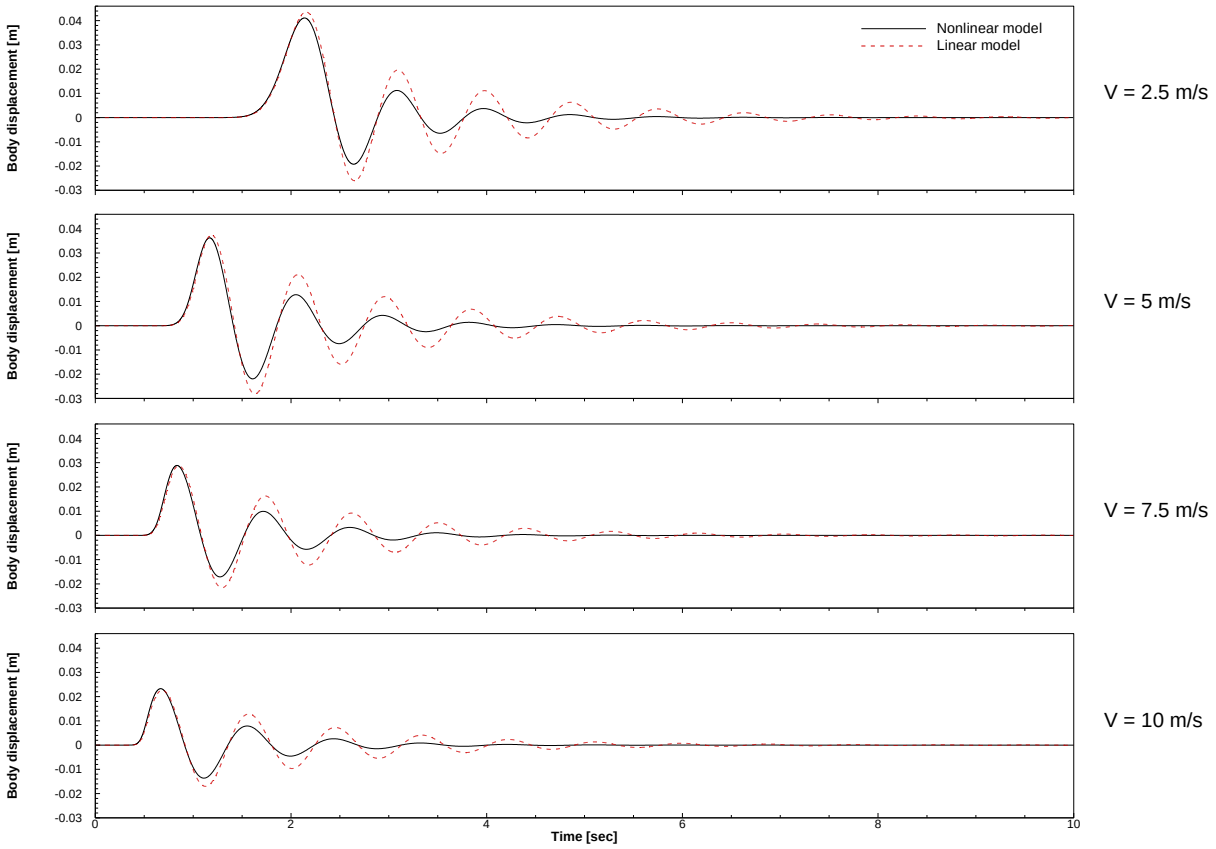

Figure 7. Vehicle body displacement (y) for bump road

more quickly. At higher velocity (5 m/s – 10 m/s) the differences between the linear and nonlinear models are still apparent, though less pronounced. The nonlinear system provides stronger damping (see **Figure 8**), while the linear system shows slightly more oscillation due to weaker damping force. The nonlinear damper response becomes stiffer as the velocity increases, preventing larger displacements while the linear system, with its constant proportional damping, struggles to control the body movement as effectively.

The damping force of the shock absorber with the linear and nonlinear model is shown in **Figure 8**. The acceleration and displacement response of the vehicle body is directly correlated with the damping force. In both the linear and nonlinear models, acceleration and displacement are directly related to the damping force. Larger body acceleration and displacements indicate insufficient damping force to control the motion effectively. In the linear and nonlinear model, the larger damping force affects the body's acceleration and displacement to reach stability at a faster rate. In the nonlinear model, the damping force increases more rapidly at certain suspension deflection velocities due to its nonlinear nature. This leads to smaller acceleration and displacement because the damper provides greater resistance as the body moves further or faster, limiting the vehicle's motion more effectively. These dynamic responses are consistent with the findings of Barethiye et al. [20], which show that the response of the linear model exhibits a more pronounced peak compared to the nonlinear model.

3.3. Vehicle Dynamics Response with Irregular Sinusoidal Road Profile

In order to analyze the dynamic response of the vehicle body with the irregular sinusoidal disturbance, four different velocities are provided. When analyzing the dynamics the figures show acceleration, displacement, and damping force with respect to time are required. Each figure has four different velocities namely, 5 m/s, 12.5 m/s, 20 m/s, and 27.5 m/s to represent the effect of vehicle speed on the vehicle dynamics response.

Figure 9 illustrates the time history of acceleration of the vehicle's body at four different speeds on an irregular sinusoidal road profile. The comparison between nonlinear and linear models

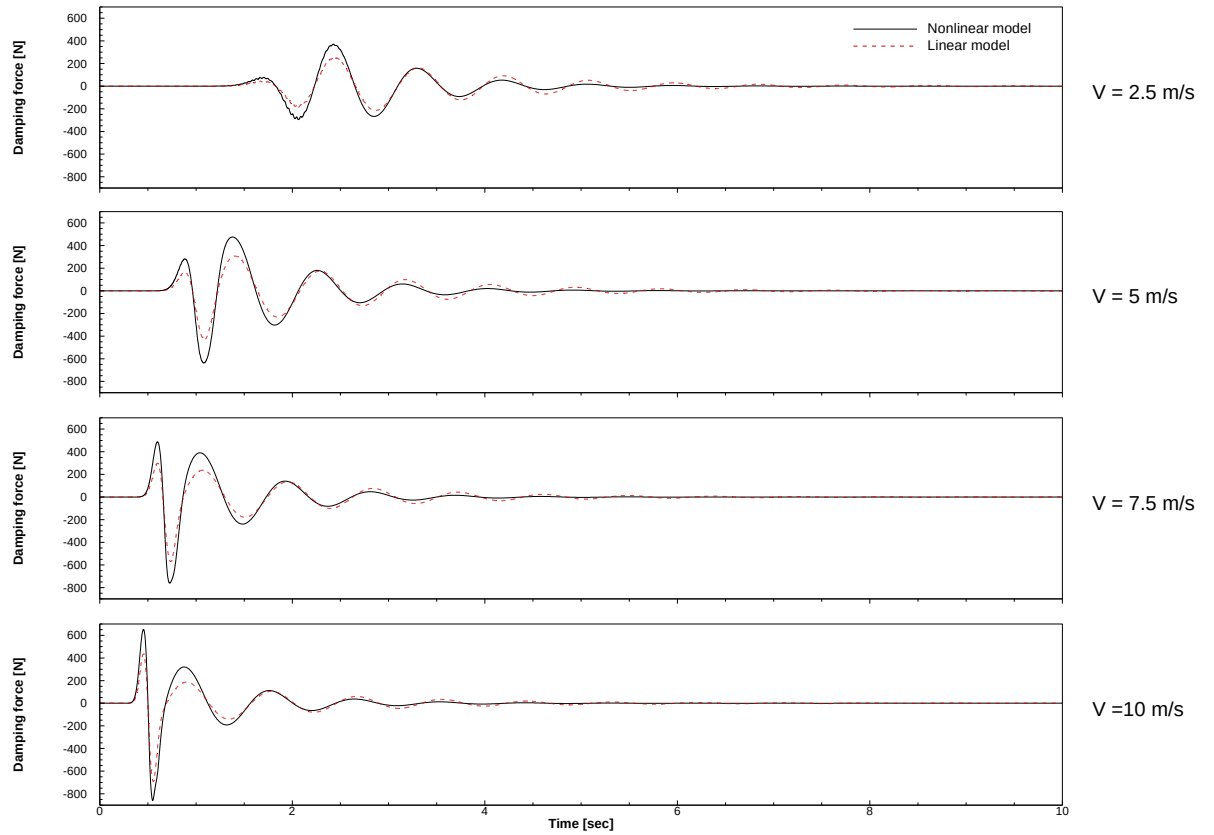

Figure 8. The damping force (F_D) of the vehicle shock absorber for bump road

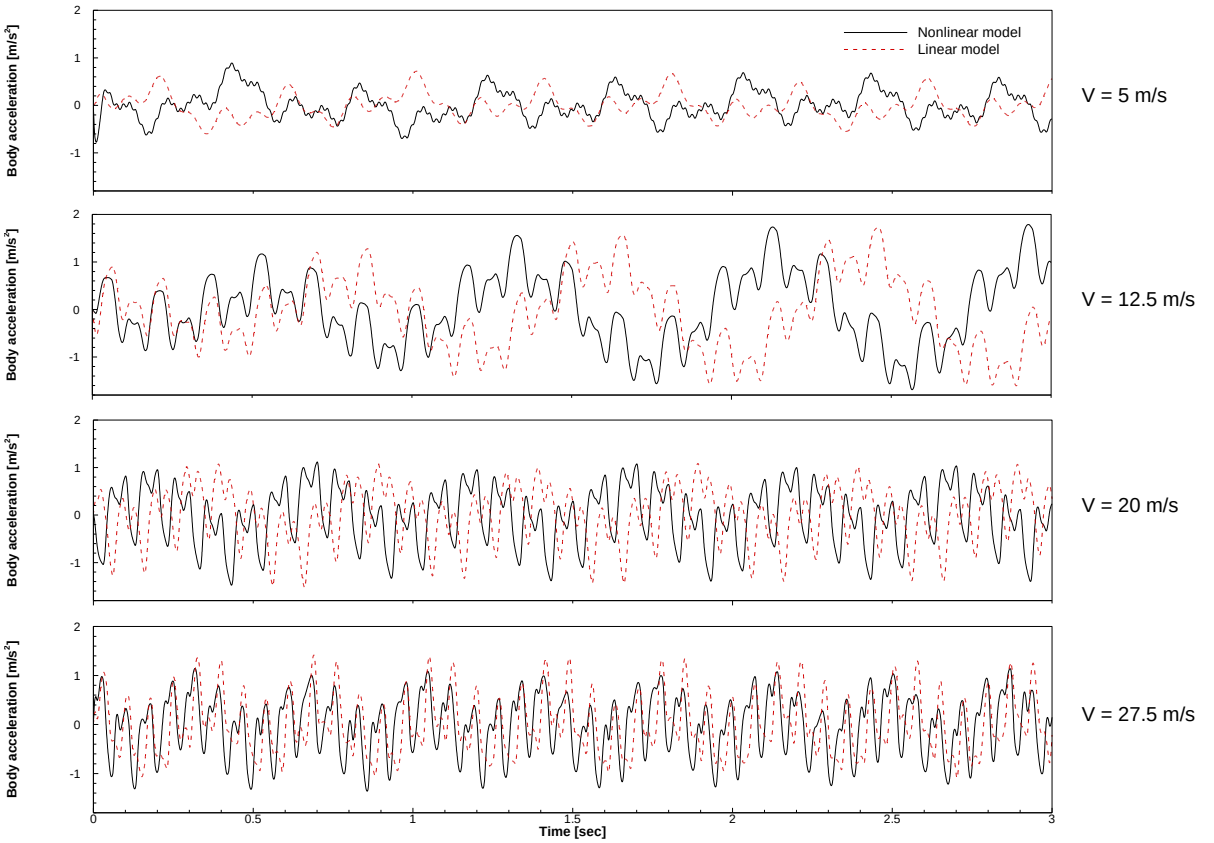

Figure 9. Vehicle body acceleration ($\ddot{y}$) for irregular sinusoidal roads

is also shown in **Figure 9**. The linear and nonlinear model acceleration response of the vehicle's body does not show any significant discrepancy. However, there is a slight discrepancy in the amplitude of the acceleration even though the discrepancy is barely visible in the **Figure 9**. This difference, though slight, is consistent across the speeds tested and suggests that the nonlinear model provides marginally better damping, particularly under conditions near resonance. The biggest discrepancy in the linear and nonlinear dynamic response is that there are significant phase shifts in the acceleration. For both linear and nonlinear models, the vehicle body acceleration shows peak amplitude at 12.5 m/s. This maximum amplitude suggests that at the speed of 12.5 m/s, the fundamental frequency of the road disturbance is close to the natural frequency of the suspension system. The closer the fundamental frequency to the natural frequency may amplify the resonance response of the vehicle body acceleration in response to the irregularities of the road profile. The drop in acceleration amplitude when the speed increases beyond 12.5 m/s indicates that as the speed increases the frequency shifts away further from the natural frequency and reduces the resonance effect. Additionally, the shock absorber also helps to moderate the resonance effect by increasing the damping force with the vehicle speed, particularly for the nonlinear model of the shock absorber.

Figure 10 displays the time history of vehicle body displacement for various speeds on irregular sinusoidal road profiles. At 5 m/s both linear and nonlinear models exhibit almost similar displacement responses with minimal difference. At this low speed, the influence of the irregularities of road disturbance is mild resulting in both models maintaining a low amplitude displacement. At 12.5 m/s the amplitude of displacement increases significantly, the displacement response consistent with the acceleration response observed at 12.5 m/s. Although the pattern is aligned with the acceleration when the speed increases beyond 12.5 m/s, the decrease in the displacement amplitude is rather more pronounced compared to the acceleration response. Meanwhile, for all the observed vehicle speeds, the nonlinear model's slightly improved damping properties help maintain lower peak responses. This relationship between displacement and acceleration reinforces

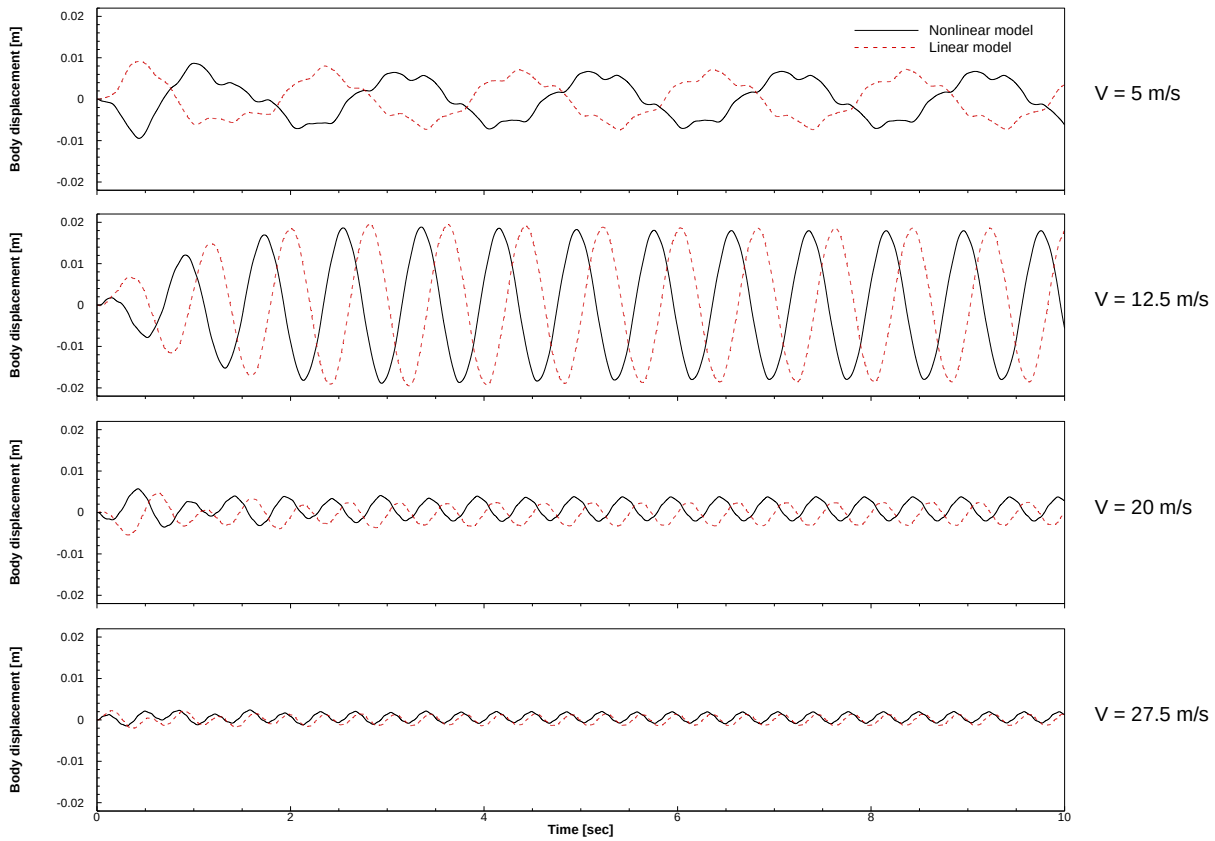

Figure 10. Vehicle body displacement (y) for irregular sinusoidal roads

the effectiveness of nonlinear passive damping, particularly at resonance, and highlights the importance of managing resonance effects for enhanced vehicle dynamics and passenger comfort.

Figure 11 shows the root mean square (RMS) values of the dynamic responses of a vehicle's body across different speeds, ranging from 5 to 30 m/s. The analysis also compares the nonlinear model (solid line with square symbol) and linear model (dashed line with circular symbol). Each graph represents different aspects of the vehicle's responses.

The RMS of body displacement (top left graph) increases with speed until it reaches a peak value of 12.5 m/s. This peak means that there is a resonance phenomenon where the vehicle's natural frequency matches with road disturbance frequency, resulting in an amplified displacement response. At speeds higher than 12.5 m/s the vehicle body displacement decreases significantly until 20 m/s. At speeds beyond 20 m/s, the body displacement responds with a less significant decrease in magnitude. This indicates that as the road disturbance frequency moves away from the natural frequency the suspension system effectively dampens the vehicle body displacement. The nonlinear model has a slightly lower displacement of RMS value particularly at the resonance speed of the vehicle where it has a larger discrepancy. This indicates that the nonlinear model has better vibration control due to its nonlinear characteristics. Similar to body displacement, the suspension deflection displays a peak value of 12.5 m/s, again highlighting the resonance effect and decreasing significantly beyond the peak value. The RMS of body acceleration shows a similar response to displacement, peaks at 12.5 m/s, and decreases with the increase in vehicle speed. However, the RMS of body acceleration shows a stabilized response indicating stability of vehicle acceleration at higher speeds. The RMS of damping force and power absorbed generally increases with speed for both models, as higher speeds generate greater suspension movement and consequently larger forces and power absorbed by the shock absorber. The damping force and power absorbed also show a marked increase of around 12.5 m/s, which corresponds to

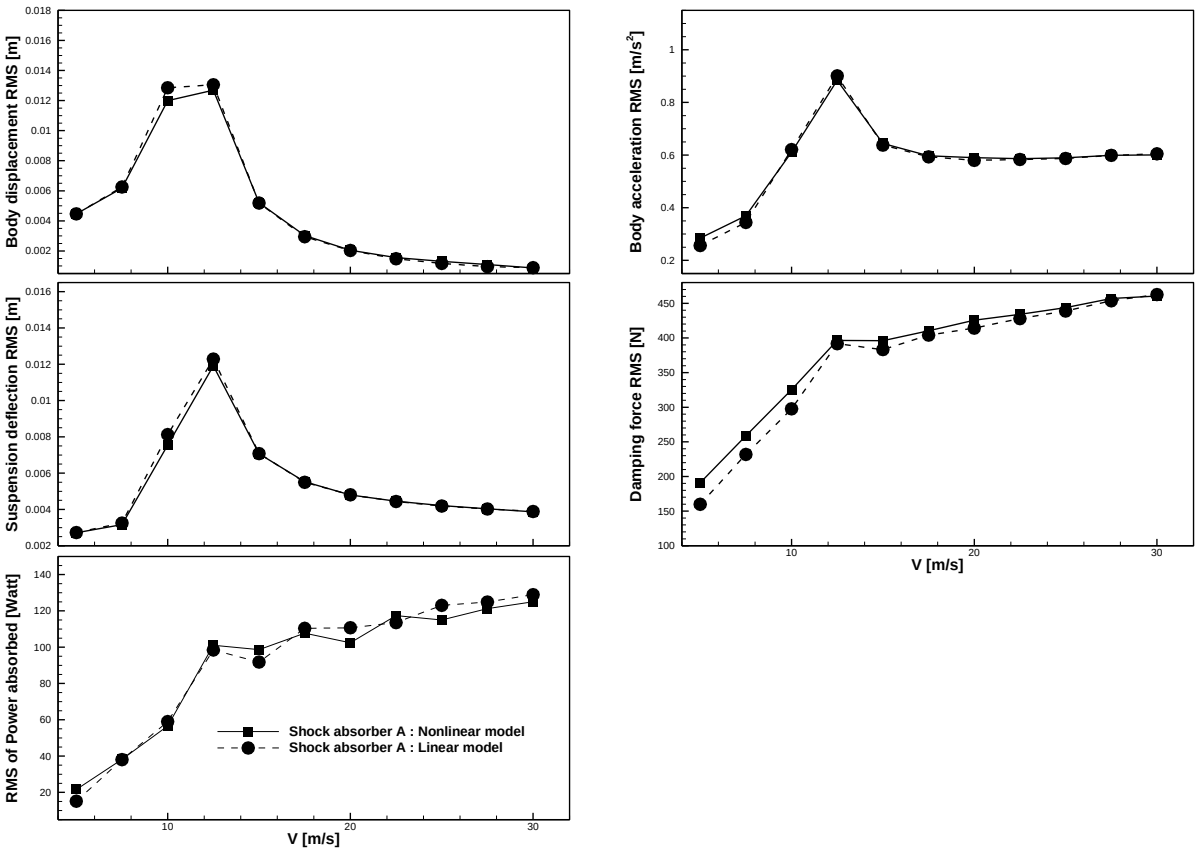

Figure 11. Root Mean Square (RMS) of the dynamics responses of the vehicle's body at each simulated vehicle speed for nonlinear (solid line) and linear (dashed line) models of a shock absorber

the increased deflection and acceleration observed at resonance. Beyond this point, they continue to increase but at a slower rate, stabilizing at higher speeds. The nonlinear model generally shows a slightly higher value of damping force compared to the linear model, especially near resonance, suggesting that the nonlinear damper exerts less force while still achieving effective damping. However, for the power absorbed, the nonlinear model absorbs slightly less power than the linear model near resonance, indicating that it is more energy-efficient at dissipating vibration-induced energy, contributing to better overall performance.

4. Conclusion

In this work, the dynamic response of a vehicle under two different road profiles—a bump and an irregular sinusoidal profile—was examined using a nonlinear shock absorber model that was developed from experimental data. A seventh-order polynomial was used to precisely represent the damping force after the experimental setting demonstrated a distinct nonlinear connection between the two variables.

In comparison to the linear model, the nonlinear shock absorber model demonstrated a closer depiction of the damping force relationship to the shock absorber deflection velocity. The necessity of non-linear formulations for vehicle dynamic simulations was highlighted by the discrepancy of linear models compared with the experimental results.

The nonlinear model showed better control over body displacement and acceleration at different vehicle speeds in the bump profile study. The capacity of the nonlinear damper to control the vehicle's reaction to sudden road abnormalities is highlighted by the nonlinear model's ability to stabilize faster than the linear model across the simulated speed.

There were minor differences between the linear and nonlinear models, as indicated by the uneven sinusoidal profile that simulated rough terrain. Due to resonance, both models showed peak responses at 12.5 m/s; however, the nonlinear model's superior damping capability was demonstrated by its lower peak displacements and accelerations. The capability of the nonlinear model in vibration control was shown by the Root Mean Square (RMS) study of vehicle responses at various speeds. It showed reduced displacement, acceleration, and suspension deflection RMS values, especially at resonance speeds.

In summary, this research underscores the importance of nonlinear shock absorber models in capturing the dynamic behavior of vehicles, especially under varied road conditions and at different speeds. Building on these findings, future research could explore the optimization of nonlinear shock absorber parameters for specific road profiles or vehicle types, investigate the integration of advanced control systems to further enhance damping efficiency, and extend the analysis to full-car models for a more comprehensive understanding of vehicle dynamics.

Acknowledgement

The authors would like to express their sincere gratitude to Pusat Penelitian dan Pengabdian kepada Masyarakat (P3M) Politeknik Negeri Semarang for the financial support provided through the Penelitian Terapan Pratama funding scheme. This support has been instrumental in facilitating the successful completion of this research. The authors appreciate the trust and commitment of P3M Politeknik Negeri Semarang in fostering research and innovation.

Author's Declaration

Authors' contributions and responsibilities

Avicenna An-Nizhami: Conceptualization of the study, development of the numerical model, and preparation of the manuscript draft. Yusuf Dewantoro Herlambang: Supervising the research methodology and ensuring adherence to standards in numerical modeling. Nanang Apriandi: Providing oversight as the principal investigator, reviewing the final manuscript, and securing research funding. Bono: Assisting in the numerical simulations and providing input on the dynamic modeling framework. Friska Ayu Fitrianti Sugiono: Statistical analysis of experimental results. Ali Sai'in: Reviewing and editing the manuscript, with a focus on technical accuracy and clarity. Ignatius Gunawan Widodo: Performing data acquisition during experiments and assisting in refining the experimental setup. Padang Yanuar: Conducting experimental tests on nonlinear passive shock absorbers and providing experimental data analysis.

Funding

P3M Politeknik Negeri Semarang through the Penelitian Terapan Pratama funding scheme.

Availability of data and materials
All data are available from the authors.

Competing interests
The authorsdeclare no competing interest.

Additional information
No additional information from the authors.

References

[1] M. P. Nagarkar, G. J. Vikhe Patil, and R. N. Zaware Patil, "Optimization of nonlinear quarter car suspension–seat–driver model," *Journal of Advanced Research*, vol. 7, no. 6, pp. 991–1007, Nov. 2016, doi: 10.1016/j.jare.2016.04.003.

[2] T. P. Phalke and A. C. Mitra, "Analysis of Ride comfort and Road holding of Quarter car model by SIMULINK," *Materials Today: Proceedings*, vol. 4, no. 2, pp. 2425–2430, 2017, doi: 10.1016/j.matpr.2017.02.093.

[3] R. E. Jonjo and S. T. Nyalloma, "Modeling the Effect of Road Excitation on Vehicle Suspension System," *International Journal of Engineering Materials and Manufacture*, vol. 5, no. 1, pp. 19–28, Mar. 2020, doi: 10.26776/ijemm.05.01.2020.04.

[4] M.-H. Jamadar, R. M. Desai, H. Kumar, and S. Joladarashi, "Analyzing quarter car model with Magneto-Rheological (MR) damper using equivalent damping and Magic formula models," *Materials Today: Proceedings*, vol. 46, pp. 9944–9949, 2021, doi: 10.1016/j.matpr.2021.02.706.

[5] J. Joshua Robert, P. Senthil Kumar, S. Tushar Nair, D. H. Sharne Moni, and B. Swarneswar, "Fuzzy control of active suspension system based on quarter car model," *Materials Today: Proceedings*, vol. 66, pp. 902–908, 2022, doi: 10.1016/j.matpr.2022.04.575.

[6] A. An-Nizhami, N. B. Sriyanto, B. Sumiyarso, S. N. Ulum, E. R. Riadini, and I. G. Widodo, "Experimental and Numerical Study of Shock Absorber Characterization and The Implication on The Dynamics of Half Vehicle Suspension System Model," *Jurnal Rekayasa Mesin*, vol. 18, no. 3, p. 409, Dec. 2023, doi: 10.32497/jrm.v18i3.5023.

[7] A. M. Kader, H. A. El-Gamal, and M. Abdelnaeem, "Influence of pneumatic tire enveloping behavior characteristics on the performance of a half car suspension system using multi-objective optimization algorithms," *Alexandria Engineering Journal*, vol. 107, pp. 298–316, Nov. 2024, doi: 10.1016/j.aej.2024.07.063.

[8] Y. L. A. Morangueira and J. C. de C. Pereira, "Energy harvesting assessment with a coupled full car and piezoelectric model," *Energy*, vol. 210, p. 118668, Nov. 2020, doi: 10.1016/j.energy.2020.118668.

[9] M. A. A. Abdelkareem *et al.*, "Energy harvesting sensitivity analysis and assessment of the potential power and full car dynamics for different road modes," *Mechanical Systems and Signal Processing*, vol. 110, pp. 307–332, Sep. 2018, doi: 10.1016/j.ymssp.2018.03.009.

[10] J. Łuczko and U. Ferdek, "Non-linear analysis of a quarter-car model with stroke-dependent twin-tube shock absorber," *Mechanical Systems and Signal Processing*, vol. 115, pp. 450–468, Jan. 2019, doi: 10.1016/j.ymssp.2018.06.008.

[11] S. K. Sharma, V. Pare, M. Chouksey, and B. R. Rawal, "Numerical Studies Using Full Car Model for Combined Primary and Cabin Suspension," *Procedia Technology*, vol. 23, pp. 171–178, 2016, doi: 10.1016/j.protcy.2016.03.014.

[12] D. Koulocheris, G. Papaioannou, and E. Chrysos, "A comparison of optimal semi-active suspension systems regarding vehicle ride comfort," *IOP Conference Series: Materials Science and Engineering*, vol. 252, p. 012022, Oct. 2017, doi: 10.1088/1757-899X/252/1/012022.

[13] P. K. Wong, W. Li, X. Ma, Z. Yang, X. Wang, and J. Zhao, "Adaptive event-triggered dynamic output feedback control for nonlinear active suspension systems based on interval type-2 fuzzy method," *Mechanical Systems and Signal Processing*, vol. 212, p. 111280, Apr. 2024, doi: 10.1016/j.ymssp.2024.111280.

[14] J. O. Pedro, S. M. S. Nhlapo, and L. J. Mpanza, "Model Predictive Control of Half-Car Active Suspension Systems Using Particle Swarm Optimisation," *IFAC-PapersOnLine*, vol. 53, no. 2, pp. 14438–14443, 2020, doi: 10.1016/j.ifacol.2020.12.1443.

[15] M. R. Abd - Elwahab, A. O. Moaaz, W. F. Faris, N. M. Ghazaly, and M. M. Makrahy, "Evaluation the New Hydro-Pneumatic Damper for Passenger Car using LQR, PID and H-infinity Control Strategies," *Automotive Experiences*, vol. 7, no. 2, pp. 207–223, Aug. 2024, doi: 10.31603/ae.10796.

[16] M. A. Khan, M. Abid, N. Ahmed, A. Wadood, and H. Park, "Nonlinear Control Design of a Half-Car Model Using Feedback Linearization and an LQR Controller," *Applied Sciences*, vol. 10, no. 9, p. 3075, Apr. 2020, doi: 10.3390/app10093075.

[17] M.-G. Unguritu, T.-C. Nichițelea, and D. Selișteanu, "Design and Performance Assessment of Adaptive Harmonic Control for a Half-Car Active Suspension System," *Complexity*, vol. 2022, no. 1, Jan. 2022, doi: 10.1155/2022/3190520.

[18] A. Armansyah, A. Keshavarzi, A. Kolahdooz, F. Ferdyanto, and M. D. Mardhani, "Optimization of air suspension system for improved ride and handling performance in road vehicles dynamic," *Mechanical Engineering for Society and Industry*, vol. 4, no. 2, pp. 277–293, Dec. 2024, doi: 10.31603/mesi.11634.

[19] Z. Hryciów, "An Investigation of the Influence of Temperature and Technical Condition on the Hydraulic Shock Absorber Characteristics," *Applied Sciences*, vol. 12, no. 24, p. 12765, Dec. 2022, doi: 10.3390/app122412765.

[20] V. Barethiye, G. Pohit, and A. Mitra, "A combined nonlinear and hysteresis model of shock absorber for quarter car simulation on the basis of experimental data," *Engineering Science and Technology, an International Journal*, vol. 20, no. 6, pp. 1610–1622, Dec. 2017, doi: 10.1016/j.jestch.2017.12.003.

[21] K. Chen, S. He, E. Xu, R. Tang, and Y. Wang, "Research on ride comfort analysis and hierarchical optimization of heavy vehicles with coupled nonlinear dynamics of suspension," *Measurement*, vol. 165, p. 108142, Dec. 2020, doi: 10.1016/j.measurement.2020.108142.

[22] J. Ke, J. He, Z. Wu, and Z. Xiang, "Fatigue reliability design of composite helical spring with nonlinear stiffness based on ply scheme design," *Composite Structures*, vol. 319, p. 117119, Sep. 2023, doi: 10.1016/j.compstruct.2023.117119.

[23] M. Silveira, P. Wahi, and J. C. M. Fernandes, "Effects of asymmetrical damping on a 2 DOF quarter-car model under harmonic excitation," *Communications in Nonlinear Science and Numerical Simulation*, vol. 43, pp. 14–24, Feb. 2017, doi: 10.1016/j.cnsns.2016.06.029.

[24] S. Mohanty and S. K. Dwivedy, "Linear and Nonlinear Analysis of Piezoelectric Based Vibration Absorber with Acceleration Feedback," *Procedia Engineering*, vol. 144, pp. 584–591, 2016, doi: 10.1016/j.proeng.2016.05.045.

[25] N. Zhang, G. Yin, T. Mi, X. Li, and N. Chen, "Analysis of Dynamic Stability of Car-trailer Combinations with Nonlinear Damper Properties," *Procedia IUTAM*, vol. 22, pp. 251–258, 2017, doi: 10.1016/j.piutam.2017.08.033.

[26] A. An-Nizhami, N. Apriandi, P. Yanuar, and W. I. Nugroho, "Pemodelan Sistem Suspensi Pasif dan Semi Aktif Regeneratif dengan Model Half Car dan Eksitasi Harmonik," *Jurnal Rekayasa Mesin*, vol. 17, no. 2, p. 297, Aug. 2022, doi: 10.32497/jrm.v17i2.3720.